JGR Solid Earth

RESEARCH ARTICLE
10.1029/2018JB017144

Aftershock Patterns in Recent Central Apennines Sequences

G. Sebastiani[1,2], **A. Govoni**[3], **and L. Pizzino**[3]

[1]Istituto per le Applicazioni del Calcolo "Mauro Picone," Consiglio Nazionale delle Ricerche, Rome, Italy, [2]Istituto "Guido Castelnuovo," Mathematics Department, "Sapienza University of Rome", Rome, Italy, [3]Istituto Nazionale di Geofisica e Vulcanologia, Rome, Italy

Key Points:
- Two different temporal patterns of aftershock migration along sequence axis were found
- The type of pattern is possibly correlated with the local lithological and hydrogeological properties

Correspondence to:
G. Sebastiani,
sebastia@mat.uniroma1.it

Citation:
Sebastiani, G., Govoni, A., & Pizzino, L. (2019). Aftershock patterns in recent central Apennines sequences. *Journal of Geophysical Research: Solid Earth*, *124*. https://doi.org/10.1029/2018JB017144

Received 13 DEC 2018
Accepted 13 MAR 2019
Accepted article online 18 MAR 2019

Abstract During the last 20 years, three seismic sequences affected the Apenninic belt (central Italy): Colfiorito (1997–1998), L'Aquila (2009), and Amatrice Visso-Norcia Campotosto (2016–2017). They lasted for a long time, with a series of moderate-to-large earthquakes distributed over 40- to 60-km-long Apenninic-trending segments. Their closeness in space and time suggested to study their aftershock sequences to highlight similarities and differences. Aftershock space migration and the distribution of aftershock interarrival times were studied. Mathematical Morphology and nonparametric statistics were applied to reduce the effect of spatial noise. Parametric analysis in time domain and spectral analysis were performed. Two different types of aftershock sequences were found. The L'Aquila sequence presented a continuous and periodic temporal variation (period ≃120 days) of aftershock activity center along the sequence axis, while the other two sequences showed a piecewise continuous pattern and a shorter duration. We also found two different types of temporal evolution of the mean radial distance between the aftershock hypocenters and the one of a reference event corresponding to the start of a large and fast increase of daily energy release. One type was well described by a simple exponential model, while a power law model was more appropriate for the other one. Furthermore, in the first case, the aftershock interarrival time was very well fitted by an exponential model, while noticeable deviations were present in the other case. A possible explanation was provided in terms of the local geological and hydrogeological properties, which depend on the region location with respect to the Ancona-Anzio tectonic lineament.

1. Introduction

The evolution of aftershock sequences are qualitatively and quantitatively influenced by many factors, for example, mainshock magnitude, tectonic setting, crustal rheology, fault properties, and fluid diffusion (e.g., Di Luccio et al., 2010; Nur & Booker, 1972; Toda & Stein, 2018; Valerio et al., 2017; Ziv, 2006). Among different features of aftershock sequences, spatial and temporal distributions of aftershock occurrence play an important role for a better understanding of the main mechanisms generating the seismic activity. For example, Valerio et al. (2017) studied duration of several aftershock sequences, finding a clear correlation with tectonic setting. In particular, they claimed that longer aftershock sequences are associated to extensional tectonic settings. Miller et al. (2004) focused on aftershock migration in the Colfiorito (1997–1998) sequence and related it to the diffusion of pressured CO_2. Malagnini et al. (2012) studied the migration of aftershocks following the largest mainshock in the L'Aquila sequence (2009). They concluded that the spatiotemporal pattern of aftershocks was influenced by a pulse of pore fluid pressure released immediately after that mainshock. Di Giovambattista and Tyupkin (2000) characterized the local weak seismicity preceding the earthquake of Colfiorito (1997–1998), which could have a relevant predictive value. Vuan et al. (2017) applied a waveform matching technique focusing on the 8-month period before the 24 August 2016 central Italy mainshock, greatly improving the catalog. Before an apparent quescience in the main fault region, they observed episodes of earthquake migration toward the mainshock nucleation zone. Caputo and Sebastiani (2011) detected a 7 days periodic pattern of foreshocks at about 3 km from the L'Aquila mainshock.

We studied here three seismic sequences that happened in the last 20 years and have affected neighboring areas of the central Apennines (Italy): the Colfiorito sequence (1997-1998), the L'Aquila one (2009), and the Amatrice Visso-Norcia Campotosto one (2016-2017). These sequences share some similarities: extensional tectonic regime, long duration (months to years), activation of more than one fault, multiple moderate to strong events close in time and space, and occurrence of thousands to tens of thousands of shocks. Our main

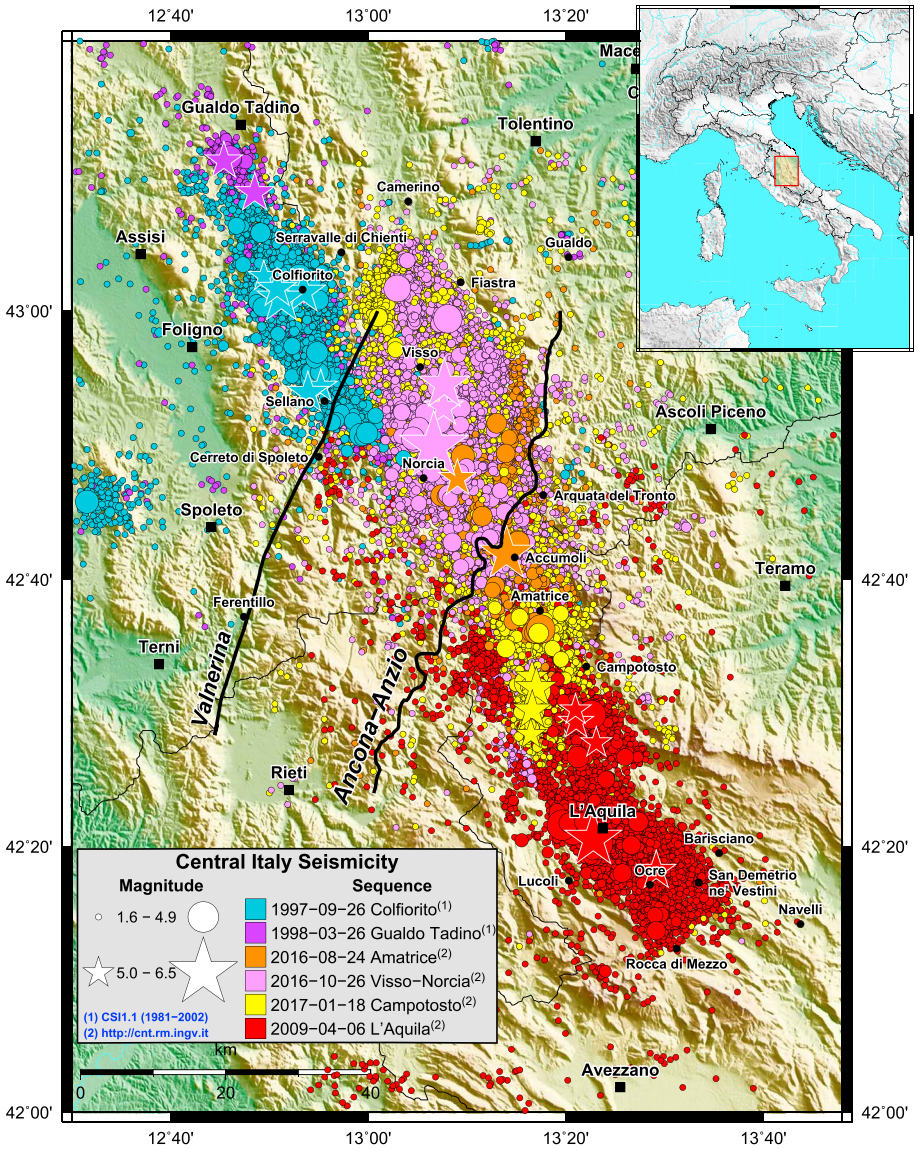

Figure 1. Epicentral map of the seismic sequences analyzed in this work. In each sequence, only events with magnitude larger than the completeness magnitude $M_c = 1.6$ are plotted using a circle ($M < 5$) or a star ($M \geq 5$). The symbol size is relatively proportional to the event magnitude. The two lines drawn in black are the Ancona-Anzio (bottom) and the Valnerina (top) thrusts.

goal was to identify similarities and differences between the three sequences. To this aim, we studied at the same time several aspects and parameters for which interesting results were already reported in the literature. However, we studied these aspects and we estimated these parameters in a different way. In particular, we focused on sequence duration and aftershock migration, both already considered in literature, and we also introduced event interarrival time. Our analysis concerned both the whole sequence and single phases. The last one is here conceived as a subsequence starting with a significant and fast increase along time of total seismic event energy, followed by a slower decrease and possibly ending with a new significant and fast increase corresponding to the start of the consecutive phase. We identified two phases for the Colfiorito sequence, one phase for the L'Aquila one, and three for the Amatrice Visso-Norcia Campotosto one. Differently from other studies (e.g., Valerio et al., 2017), the duration of aftershocks was quantified here by means of a statistically based method. The evolution of aftershock spatial distribution was studied with or without taking into account the evident strong spatial anisotropy of the three considered sequences. Parametric temporal models were adopted to describe the evolution of aftershock spatial distribution. In the case of

Table 1
Some Basic Information About the Three Seismic Sequence Data Sets Analyzed in This Work

Sequence phase	Phase reference event	Spatial window ulc	Spatial window lrc	Time window Start	Time window End	No. of shocks
Colfiorito	1: 1997/09/26 M_w 5.7	(43.4,12.5)	(42.7,13.3)	1997/08/26	1999/08/25	9,427
	2: 1998/04/03 M_w 5.1					
L'Aquila	3: 2009/04/06 M_w 6.3	(42.85,12.9)	(41.85,13.9)	2008/12/01	2012/04/06	29,009
Amatrice	4: 2016/08/24 M_w 6.0	(43.2,12.8)	(42.2,13.8)	2016/07/01	2018/01/25	82,021
Visso-Norcia	5: 2016/10/26 M_w 5.4					
Campotosto	6: 2017/01/18 M_w 5.1					

Note. The criteria adopted to select the values of the spatial and temporal windows, as well as those of the starts of the phases of the sequences, will be illustrated in section 3.2. The acronym ulc (lrc) stands for upper left (lower right) corner. Dates are formatted as YYYY/MM/DD.

periodic pattern, frequency domain analysis was also performed. Nonparametric statistical techniques and Mathematical Morphology were applied to reduce the effect of noise. Hierarchical clustering was used to identify groups from the results of the event interarrival time analysis.

At sequence level, two main patterns for the migration of aftershocks were found: one continuous and periodic and the other one piecewise continuous. Furthermore, the first one was associated with longer sequence duration than the other one. Concerning the analysis of single phases, two different behaviors were observed. In addition, the behavior was associated to some features of the interarrival time distribution. The different sequence and sequence phase behaviors were possibly related to the lithological and hydrogeological setting of the areas where the aftershocks occurred, which depends on the area location with respect to the NE-SW Ancona-Anzio tectonic lineament.

2. Seismic Data Description

In this section, we describe the main features of the three seismic sequences data sets selected in this study. Figure 1 shows the epicentral map of the sequences analyzed here. The catalog data used in this study is provided by the Istituto Nazionale di Geofisica e Vulcanologia (INGV) web services: ISIDe working group (2016) version 1.0 (https://doi.org/10.13127/ISIDe) that is accessible at http://cnt.rm.ingv.it/en/iside website. The Colfiorito sequence data were extracted from the CSI 1.1 (1981–2002) catalog (Castello et al., 2006), available at http://csi.rm.ingv.it/ website. In Table 1, some basic information about the three data sets are shown. The criteria adopted to select the values of the spatial and temporal windows, as well as those of the starts of the sequence phases, will be illustrated in section 3.2.

2.1. The Colfiorito Sequence

From September 1997 to April 1998 a long sequence of earthquakes, eight with M_w between 5 and 6 (three with $M_w > 5.5$), struck central Italy in the Colfiorito area. It caused severe damages and loss of human lives, despite that earthquakes did not occur close to any large towns (Chiaraluce et al., 2004, and references therein). The first event occurred on 3 September with $M_w = 4.5$, followed by aftershocks for 3 weeks approximately (Ripepe et al., 2000). The strongest shocks ($M_w > 5.5$) occurred

(i) on 26 September at 00:33 UTC ($M_w = 5.7$) at about the same location of the 3 September event;
(ii) on 26 September at 09:40 UTC ($M_w = 6.0$), 3 km W-NW of (i); and

Table 2
Aftershock Duration for the Three Sequences Analyzed Here

Sequence	Aftershock duration	Aftershock duration (Valerio et al., 2017)
L'Aquila	520 days	515 days
Amatrice Visso-Norcia Campotosto	320 days	—
Colfiorito	310 days	330 days

Note. The values estimated in Valerio et al. (2017) are also shown.

(iii) on 14 October at 15:23 UTC ($M_w = 5.6$), near the village of Sellano, far away from the other shocks.

Up to 31 December 1997, seismicity was characterized by more than 25 earthquakes with $M_l > 4.0$ and about 1,000 earthquakes with $M_l > 2.0$ (Barba & Basili, 2000). Earthquakes occurred over a NW-SE elongated zone approximately 40 km long and extending for 5 to 15 km in the perpendicular direction (Amato et al., 1998).

The focal mechanisms of the largest shocks revealed normal faulting with NE-SW extension perpendicular to the trend of the Apennines, consistently with the Quaternary tectonic setting of the internal sector of the belt and with previous earthquakes in adjacent regions (Chiaraluce et al., 2004). Moreover, the patterns of the spatial distribution of both aftershocks and damage also suggest that the three main shocks ruptured distinct 5- to 15-km-long fault segments, adjacent and slightly offset from one another.

Another significant event occurred on 3 April 1998 ($M_w = 5.1$), 5 km SW of Gualdo Tadino town, at about 15 km NW of Colfiorito area (Ciaccio et al., 2005). This additional event and its aftershocks (about 200 in the first week after the mainshock, with M_d in the range 1.05–4.52) identified a NW-SE elongated and 8-km-long ruptured fault, parallel to the Colfiorito fault segments (Ciaccio et al., 2005). This event increased the overall extent of the seismogenic area along the Apenninic chain to more than 60 km. The Gualdo Tadino event was preceded on 26 March 1998 by a subcrustal $M_w = 5.3$ earthquake, which was located at 48-km depth, likely related to the bending of the Adriatic lithosphere beneath the Apenninic belt (Selvaggi & Amato, 1992).

The spatiotemporal evolution of the 1997-1998 sequence has several similarities with those that occurred in the eighteenth century, both to the north and to the south of the Colfiorito area (Deschamps et al., 2000; Galli & Galadini, 1999). These seismic sequences (1279, 1703, 1730, and 1747–1951) indicate that an entire fault system may be activated in two different ways. In the first one, rupture may happen by a single event with $M_w \geq 6.5$. Alternatively, seismic crises can be due to the break of multiple small faults; in this case, sequences may last many months as for the 1997–1998 one with a clear migration of seismicity along the entire portion of the activated fault system.

In our analysis, we divided this sequence in two phases, as follows. The first one started with the event named 1 on 26 September 1997, while the second one began with event named 2 on 3 April 1998 (see Table 1). This choice was motivated by a quantitative criterion, based on seismic event daily energy, as shown in section 3.2. The event of 26 March 1998 was ignored in our analysis because of its subcrustal depth (48 km), completely outside of the depth range of the Colfiorito area events. The first phase ended one week before the beginning of the following one.

2.2. The L'Aquila Sequence

On 6 April 2009 (01:32 UTC, latitude 42.342, longitude 13.380), a $M_w = 6.3$ earthquake struck central Italy causing 308 deaths and leaving around 65,000 homeless. The earthquake caused considerable damage to structures over a very wide area, devastating the L'Aquila town and several villages. The main event had a pure normal faulting mechanism; its location was set at 9.5-km depth and at distance of about 2 km from the center of the L'Aquila town.

The 6 April 2009 main shock was preceded by a long sequence of foreshocks, which started in October 2008, culminating with a $M_l = 4.1$ shock on 30 March (13:38 UTC, latitude 42.321, longitude 13.376). During the last 3 months before the 6 April mainshock, a cluster of small magnitude earthquakes with 7 days periodic pattern occurred with center at about 3 km from the mainshock location (Caputo & Sebastiani, 2011). A few hours before the main event, a $M_w = 3.9$ (5 April at 20:48 UTC, latitude 42.325, longitude 13.382) and a $M_w = 3.5$ (5 April at 22:39 UTC, latitude 42.329, longitude 13.385) foreshocks occurred.

The strongest ($M_w = 5.4$) aftershock of the sequence struck on 7 April at 17:47 UTC; its focal mechanism displayed a nonnegligible strike-slip component. This event occurred a few kilometers to the south of the main event, at a depth of 17 km and was followed by a few aftershocks. The mainshock rupture activated a NW-SE trending, 15- to 18-km-long fault. In the first 3 days after the main event, seismicity migrated from the main structure northward. In fact, three large events took place on 6 April ($M_w = 5.0$ at 23:15 UTC) and 9 April ($M_w = 5.2$ at 01:52 UTC and $M_w = 5.0$ at 20:38 UTC), located in the Pizzoli-Capitignano-Campotosto area. On 13 April, another event ($M_w = 4.8$ at 21:14 UTC) occurred in the same area. The focal mechanisms of these four events showed a pure normal solution. During the following months, seismicity spread along a 40-km-long fault system, showing an Omori-like temporal decay. Aftershock data with more than 46,000

events (Chiaraluce et al., 2011; Valoroso et al., 2013) were relocated to provide an extraordinary resolution of the geometry of the faulting.

In this case, the sequence was composed of a single phase starting with the event named 3 on 6 April (M_w = 6.3; see Table 1).

2.3. The Amatrice Visso-Norcia Campotosto Sequence

In 2016–2017, central Italy experienced one of the most important seismic sequences that ever took place in the country. A series of moderate-to-large earthquakes activated a 80-km-long Apenninic-trending normal-fault system. Up to now, more than 100,000 events have been recorded by the seismic network of the INGV (ISIDe working group, 2016). The first strong event occurred on 24 August (01:36 UTC, M_w = 6.0) and ruptured two distinct segments of this fault system, corresponding to the northern part of the ~50° SW dipping Monte Gorzano fault and to the southern part of the ~40° SW dipping Monte Vettore fault, respectively (see, e.g., Chiaraluce et al., 2017). This event, whose epicenter was located only 1 km from the Accumoli village and just 9 km from the Amatrice town, caused 299 fatalities and more than 20,000 homeless, partially destroying these towns and their hamlets. Extensive damage were reported in a wide area relative to four administrative regions. It was the largest earthquake, together with the 1703 one, to strike this portion of central Apennines since the 7 October 1639 (estimated macroseismic magnitude = 6.2), earthquake (CPTI15, Rovida et al., 2016), considered a twin of the 24 August one (Galli et al., 2016).

No significant foreshocks were recorded. The seismicity rate did not show significant variations during the 4 years before the mainshock, and seismicity appeared rather uniformly distributed in both time and space, within an area centered at the 24 August epicenter (Marzorati et al., 2016). In contrast, other authors pointed out a seismic quiescence, started since the beginning of September 2015, in the area where the mainshock occurred (Gentili et al., 2017). Even more interesting, Vuan et al. (2017) applied a waveform matching technique focusing on the 8-month period before the 24 August 2016 central Italy mainshock, greatly improving the catalog. Before an apparent quescience in the main fault region, they observed episodes of earthquake migration toward the mainshock nucleation zone.

Almost 1 hr after the mainshock, an aftershock of M_w = 5.3 occurred, located close to the Norcia town, 12 km NW of the mainshock. The following seismic sequence was characterized by several aftershocks located SE and NW of the epicenter (Chiaraluce et al., 2017). They decreased in frequency and magnitude until the 26 October, when two earthquakes, M_w = 5.4 (at 17:10 UTC) and M_w = 5.9 (at 19:18 UTC), occurred. They enucleated at the northernmost extent of the sequence and were located between Visso and Ussita, about 25 km NW of the 24 August mainshock. The M_w = 5.9 event occurred on a ~40° SW dipping, 15-km-long fault, belonging to the Monte Vettore tectonic system.

On 30 October (06:40 UTC), a third large event of magnitude M_w = 6.5 enucleated beneath the town of Norcia, rupturing the ~20-km-long segment that had remained unbroken after the previous large events. The fault geometry was consistent with a 47° SW dipping main normal fault belonging to the Monte Vettore-Monte Bove fault system (Scognamiglio et al., 2018). This event was the largest recorded in Italy since 23 November 1980 Irpinia M_s = 6.9 earthquake (Gasparini et al., 1993).

Finally, on 18 January 2017, a series of four major earthquakes, all with magnitude ≥ 5, (09:25 UTC, M_w = 5.1), (10:14 UTC, M_w = 5.5), (10:25 UTC, M_w = 5.4), and (13:33 UTC, M_w = 5.0) took place in the Campotosto-Pizzoli area, extending to the SE the seismogenic volume. These earthquakes were followed by multiple aftershocks. The fault mechanism of the four shocks pointed out a pure normal faulting, with a NE-SW extension, in agreement with the predominant regime characterizing the central Apennines. Only in the event of M_w = 5.0, a remarkable strike-slip component was present.

In our analysis, we divided this sequence in three phases, as follows. The first one started with the event named 4 on 24 August, the second phase began with the event named 5 on 26 October, and the last one started with the event named 6 on 18 January (see Table 1). This choice was motivated by a quantitative criterion, based on seismic event daily energy, as shown in section 3.2. Each of the first two phases ended 1 week before the beginning of the following one.

2.4. Completeness Magnitude

For each sequence data set, the value of the completeness magnitude was computed as follows. Based on all sequence events (including all phases) since the reference event of the first sequence phase (see Table 1),

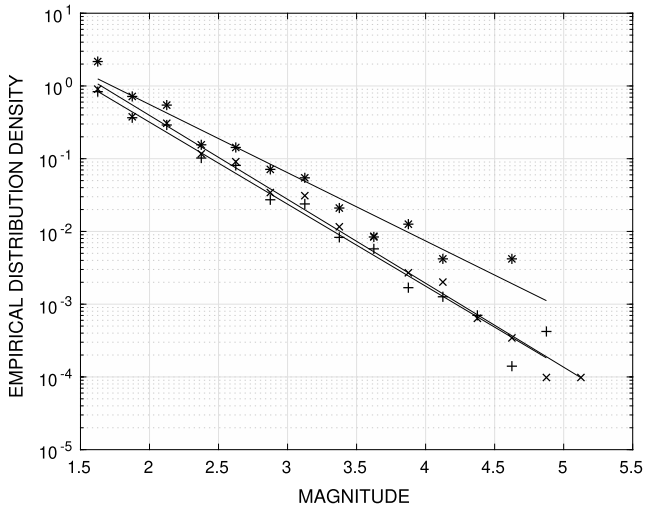

Figure 2. Empirical distribution density of the event magnitude estimated for the three sequence data sets (+: L'Aquila; ×: Amatrice Visso-Norcia Campotosto; ⋆: Colfiorito). The three data best linear fits are also superimposed.

we first computed the empirical distribution density of the magnitude in the interval $[0, 7]$ discretized in 28 bins of length 0.25. Then, a linear fit was performed between the empirical distribution density values logarithmically transformed and the corresponding bin central values. The fitting procedure was repeated many times for different windowing of the magnitude values, corresponding to all possible choices of the window left and right points in the bin sets $\{1, 2, \ldots, 9\}$ and $\{20, 21, \ldots, 28\}$, respectively. Among all possible fits, we selected the one corresponding to the highest correlation coefficient (in absolute value) between the windowed empirical distribution density values (logarithmically transformed) and the corresponding bin central values. Pairs with null value of the empirical distribution density were excluded. The value of the completeness magnitude was then set equal to the central value of the left bin of the selected window. When there was more than one window selected, the one with the smallest value of the left point was chosen.

Values of the completeness magnitude were the same for the three sequences, equal to 1.6. In Figure 2, the fits selected for the three sequences are shown superimposed to the corresponding empirical distribution densities. Fits corresponding to the data sets of L'Aquila and Amatrice Visso-Norcia Campotosto were almost coincident; this is probably due to the closeness in time of the two sequences, which were therefore measured by networks with similar features. Although the Colfiorito sequence seems to have a slightly different b value and to be more noisy, it is remarkable that the completeness magnitude value of the three sequence data sets were identical.

3. Data Analysis Methods

3.1. Aftershock Duration

The duration of aftershock sequence was estimated using the whole catalog data used for each of the three sequences starting from the associated mainshock (with no knowledge of the phases).

For each sequence, we have first chosen as temporal origin the time of the reference event (see Table 1). Then, we computed the temporal sequence $\mathbf{N}{:=}N_1, N_2, \ldots, N_{T_s}$ of the number of events with magnitude above the completeness magnitude of that sequence happened every consecutive 24 hr, where T_s is the total number of days considered from the temporal origin of above. Based on the sequence $\mathbf{N}$, the length of the aftershock sequence was determined here as follows. We generated two subsequences with same length T. One of them $\bar{\mathbf{N}}{:=}N_{T_s-T+1}, \ldots, N_{T_s}$ was fixed and contained the last T values of the sequence $\mathbf{N}$. Instead, the other one, $\bar{\mathbf{N}}_t$, was not fixed and was obtained extracting T consecutive values in all possible ways from the first $T_s - T$ values of $\mathbf{N}$, that is, $\bar{\mathbf{N}}_t := N_t, \ldots, N_{t+T-1}$. In this way, the two subsequences $\bar{\mathbf{N}}_t$ and $\bar{\mathbf{N}}$ did never intersect to each other. We then computed the mean value μ (μ_t) and variance S^2 (S_t^2) of the subsequence $\bar{\mathbf{N}}$ ($\bar{\mathbf{N}}_t$). From the values μ and S^2, and the sequences $\mu_1, \mu_2, \ldots, \mu_{T_s-2T+1}$ and $S_1^2, S_2^2, \ldots, S_{T_s-2T+1}^2$, we obtained the sequence $w_1, w_2, \ldots, w_{T_s-2T+1}$ of a statistics commonly used to test significance of mean values difference:

$$w_t = \frac{\bar{\mu}_t - \bar{\mu}}{\sqrt{\frac{S_t^2 + S^2}{T}}}. \tag{1}$$

If the sample size T is large enough, under the null hypothesis that there is no difference, the statistics w_t can be well approximated by a $N(0, 1)$ Gaussian random variable (Lehmann, 1998). Therefore, we set the aftershock duration equal to the first time t' such that $w_t \leq 3$, $\forall t \geq t'$, which corresponds to at least a 0.999 significance level of the test. The value of T was chosen as the largest one that allowed to detect in a clear way the end of the aftershock sequence.

3.2. Aftershock Spatial Distribution Evolution

The analysis of aftershock migration was performed in two different ways.

In the first one, as done for standard diffusion, given a reference event of the considered sequence phase (see Table 1), the three-dimensional euclidean distance d_k between its hypocenter and the one of the kth

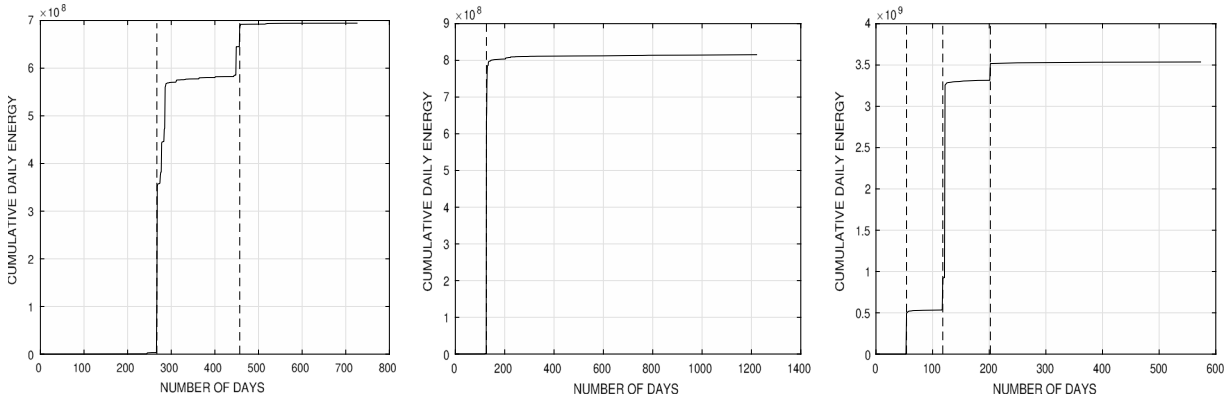

Figure 3. The cumulative curve of the total daily energy E based on events with magnitude above the completeness magnitude value for the sequence data sets of Colfiorito (left), L'Aquila (center), and Amatrice Visso-Norcia Campotosto (right). The vertical bars correspond to the jumps of the cumulative curve and were chosen as starting point of the sequence phases.

event was computed. Then, every 24 hr since the time of the reference event, the daily weighted mean value $\mathrm{d}(t)$, $t = 1, 2, \ldots$ of this distance was computed based on all events in that temporal interval whose magnitude was above the completeness magnitude value M_c of the sequence under study:

$$\mathrm{d}(t) = \sum_{k|M_k>M_c,\, t-1\le t_k/T_D<t} d_k \cdot E_k^{1/4}/q(t), \tag{2}$$

where t_k is the number of seconds elapsed at occurrence of event k since the reference event and T_D is the length of a day in seconds. The used weights $E_k^{1/4}/q(t)$ were the normalized fourth root of the event energies ($q(t)$ was the normalizing constant), computed using the empirical relation

$$E = 10^{[1.44M+5.24]}, \tag{3}$$

where E is in joules (Bath & Duda, 1964) and M is the event magnitude. Then, two different types of parametric models were used for the temporal sequence of the daily weighted mean distance $\mathrm{d}(t)$ ($t = 1, 2, \ldots$).

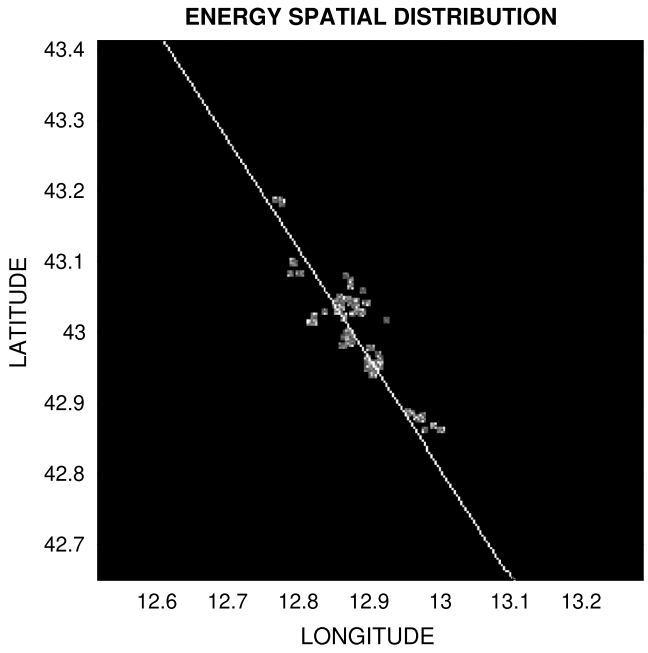

Figure 4. The spatial distribution of the fourth root of the energy E for all events of the Colfiorito sequence data set with magnitude above the completeness magnitude value. The straight line corresponds to the best linear fit between longitude and latitude values of events with magnitude larger than 4.0.

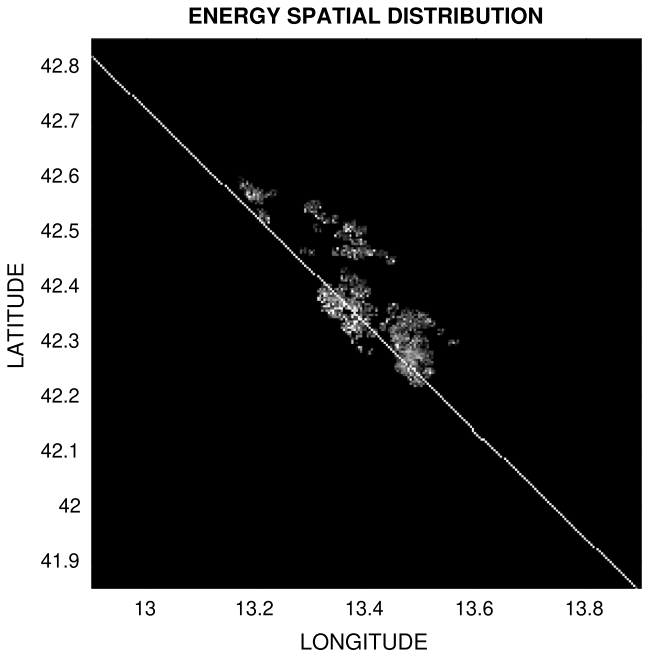

Figure 5. The spatial distribution of the fourth root of the energy E for all events of the L'Aquila sequence data set with magnitude above the completeness magnitude value. The straight line corresponds to the best linear fit between longitude and latitude values of events with magnitude larger than 4.0.

The first one was exponential: $\mathrm{d}(t) = d_\infty \cdot (1 - \exp(-t/\tau))$, while the other one was a power law: $\mathrm{d}(t) = \mathrm{d}' \cdot t^\alpha$, where all parameters of the two models were positive. As anticipated before, the times chosen for the sequence phase starts were chosen as the jumps in the temporal sequence of the daily energy E of all sequence events with magnitude above the completeness magnitude value. This can be appreciated in Figure 3. To reduce the effect of random fluctuations, the cumulative curve of the daily energy sequence was used. From this figure, we can also evidence that the temporal windows chosen for the whole sequence data sets were appropriate.

Instead, the second approach was based on the fact that the energy spatial distribution was concentrated along an axis. In Figures 4–6, we show the spatial distribution of the fourth root of the energy E for the events of Colfiorito, L'Aquila, and Amatrice Visso-Norcia Campotosto sequence data sets, with magnitude above the completeness magnitude value. The closing operator of Mathematical Morphology was applied to reduce the effect of spatial noise (Serra, 1982). The straight lines correspond to the best linear fits between longitude and latitude values of events with magnitude larger than 4.0 and will be used afterward as sequence axes. As anticipated at the beginning of section 2, we illustrate now the criterion used here to select the values of the widths of the spatial windows of the sequence data sets. First of all, the selected width values correspond to regions of about 100 km ×100 km, which are known to be large enough to collect the aftershocks of sequences in central Apennines. Furthermore, the spatial distribution of the fourth root of the energy E of all events with magnitude above the completeness magnitude value projected along the sequence axis, shown in Figure 7, has negligible values in the window external parts.

Also for this approach, a reference event was considered for each sequence: events named 1, 3, and 4 for the Colfiorito, L'Aquila, and Amatrice Visso-Norcia Campotosto sequence data sets, respectively (see Table 1). Then, for each temporal interval $t = 1, 2, \ldots$ of length 24 hr following the reference time, we computed a center of daily aftershock activity $c(t)$ along the axis, as follows. After discretizing the axis, we computed at each axis point i, the weighted average value $E_i(t)$ of the fourth root of energy based on every event k of that day whose magnitude was above the completeness magnitude M_c of the considered sequence and whose epicenter $\mathcal{P}_k$ was within a circle R_i with radius r centered at i:

$$E_i(t) = \sum_{k|M_k>M_c,\, t-1\le t_k/T_D<t,\, \mathcal{P}_k\in R_i} E_k^{1/4} \exp[-.5(2.5\, d_{ki}/r)^2]. \quad (4)$$

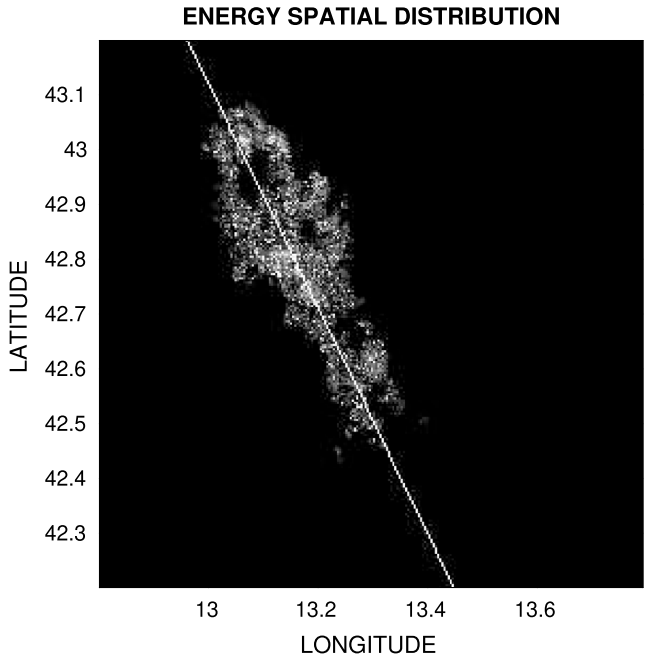

Figure 6. The spatial distribution of the fourth root of the energy E for all events of the Amatrice Visso-Norcia Campotosto sequence data set with magnitude above the completeness magnitude value. The straight line corresponds to the best linear fit between longitude and latitude values of events with magnitude larger than 4.0.

As commonly done in nonparametric regression, the weights used were exponentially Gaussian decreasing with the euclidean distance d_{ki} between $\mathcal{P}_k$ and the axis point i (Hastie & Tibshirani, 1990). The Gaussian standard deviation was set to $r/2.5$. The value of the circle radius r was chosen based on the maximum linear dispersion of the energy spatial distribution across the axis. Then, for each day $t = 1, 2, \ldots$, the center of aftershock activity along the sequence axis $c(t)$ was computed as the mean value of the latitude l of the axis point, weighted by the average value $E_i(t)$ of the fourth root of energy in that day at the same point.

$$c(t) = \frac{\sum_i l_i E_i(t)}{\sum_i E_i(t)}. \tag{5}$$

Then, for each main activity phase, $c(t)$ was modeled as for the first approach. However, for the L'Aquila sequence there was only one main activity phase, and in this case a simple parametric sinusoidal model was more appropriate. Alternatively, nonparametric analysis in the frequency domain could be performed. This was done by using the classical periodogram (Schuster, 1906). For both parametric and nonparametric

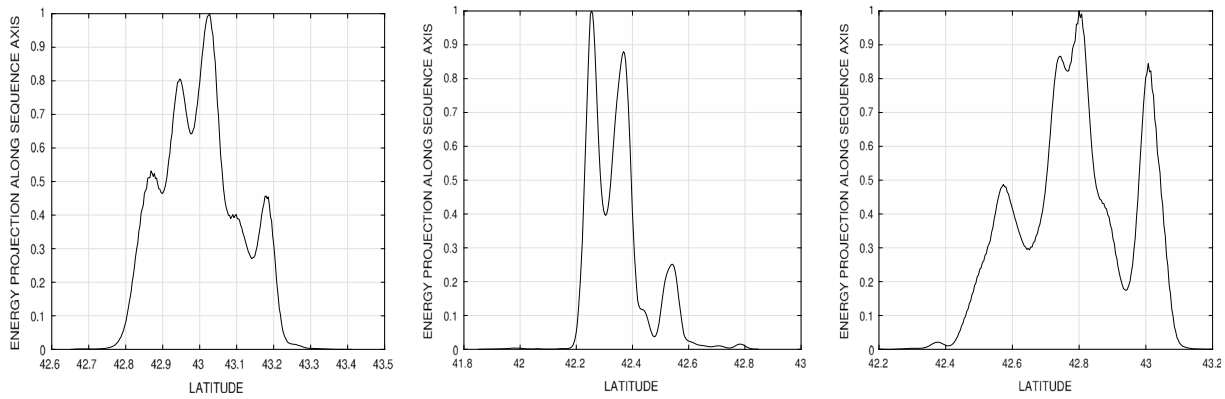

Figure 7. The projection along the axis of the Colfiorito (left), L'Aquila (center), and Amatrice Visso-Norcia Campotosto (right) sequence data sets of the corresponding spatial distributions of the fourth root of the energy of all sequence events with magnitude above the completeness magnitude value.

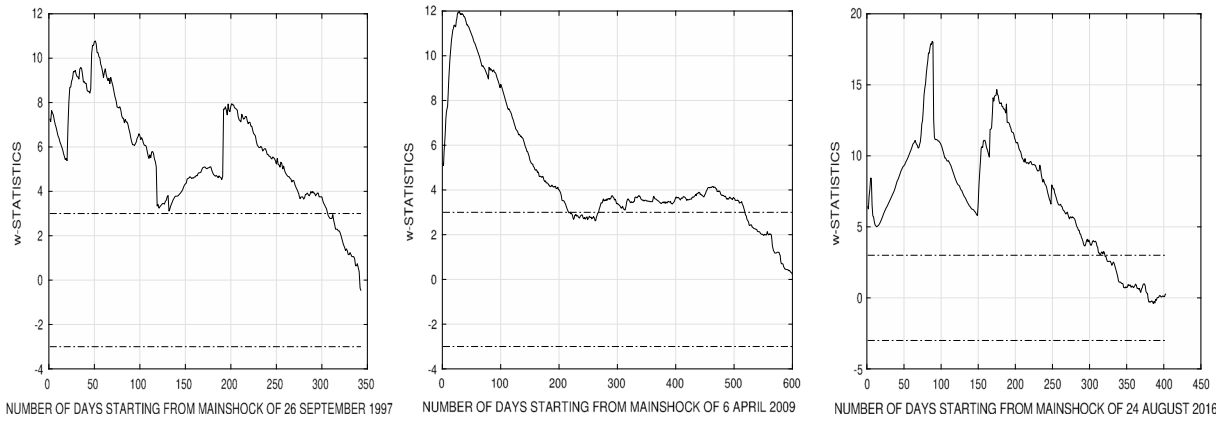

Figure 8. The values of the w-statistics as in equation (1) versus the time starting since the reference event (see Table 1) of the Colfiorito (left), L'Aquila (center), and Amatrice Visso-Norcia Campotosto (right) sequence data sets. The dashed horizontal lines correspond to the threshold value set to 3, and the values shown in Table 2 correspond to the first times after which the curves remain always below the threshold.

approaches, the number of days used was made to vary in a finite set of values. By minimizing the mean square error between data and model, the value of this number was found for the parametric approach. Instead, the ratio between the strength of the two largest peaks of the periodogram was maximized for the nonparametric approach.

3.3. Aftershock Interarrival Time Distribution

Similarly to the previous analyses, for each activity phase of a sequence, a reference event was considered: events named 1, 3, and 4 for the Colfiorito, L'Aquila and Amatrice Visso-Norcia Campotosto sequence data sets, respectively (see Table 1). Then, the set $\mathcal{T}$ of the times between consecutive events within 12 hr since the reference one and whose magnitude was larger than the completeness magnitude value, was computed. Theoretically, for the classical Poisson process, one can prove that the event interarrival time density function is exponentially decreasing, as well as the survival function (Daley & Vere-Jones, 2003). We recall that the survival function of a nonnegative random variable evaluated at any non negative real value is the probability that the random variable is larger than that value. Saichev and Sornette (2007) and Spassiani and Sebastiani (2016) derived theoretically asymptotic expressions for the distribution of interarrival time for two versions of the Epidemic Type Aftershock Sequence model. Furthermore, Molchan (2005) derived theoretically the exponential model for the interarrival time density, under very general conditions. Therefore, in logaritmic scale the survival function should be well described by a decreasing straight line. The choice of using the value 12 hr for the length of the considered time interval was a compromise between the need of having a sufficiently high number of events and that of observing the behavior at small time scale. As expected theoretically, we verified that the exponential model fitted very well the data when the time interval was sufficiently long, for example, a few days. For each activity phase, the survival function was evaluated between the minimum value of the set $\mathcal{T}$, and its mean value plus three times its standard deviation. For each of the six activity phases, we estimated the normalized mean square error between the logarithm of the estimated survival function and its best linear model fit, together with the proportionality constant of the best linear fit. Hierarchical clustering (Ward, 1963) was then applied to the values of this pair of variables estimated for the six activity phases. The clustering algorithm was driven by the Ward criterion, which minimizes the sum of intracluster variances, computed on the basis of the Euclidean distance.

4. Results

4.1. Duration of Aftershocks

In a recent paper (Valerio et al., 2017), it was provided evidence of a dependence between aftershock duration and tectonic style, that is, extensional or compressive. In particular, these authors found out a longer duration of seismic sequence associated to normal faulting. All the three sequences studied here were of extensional type; as such, we estimated their aftershock duration to see if there were differences among them. In Figure 8, we show the values of the w-statistics in equation (1) versus the time since the reference event of the three sequences (in each plot, the dashed horizontal line corresponds to the threshold value set

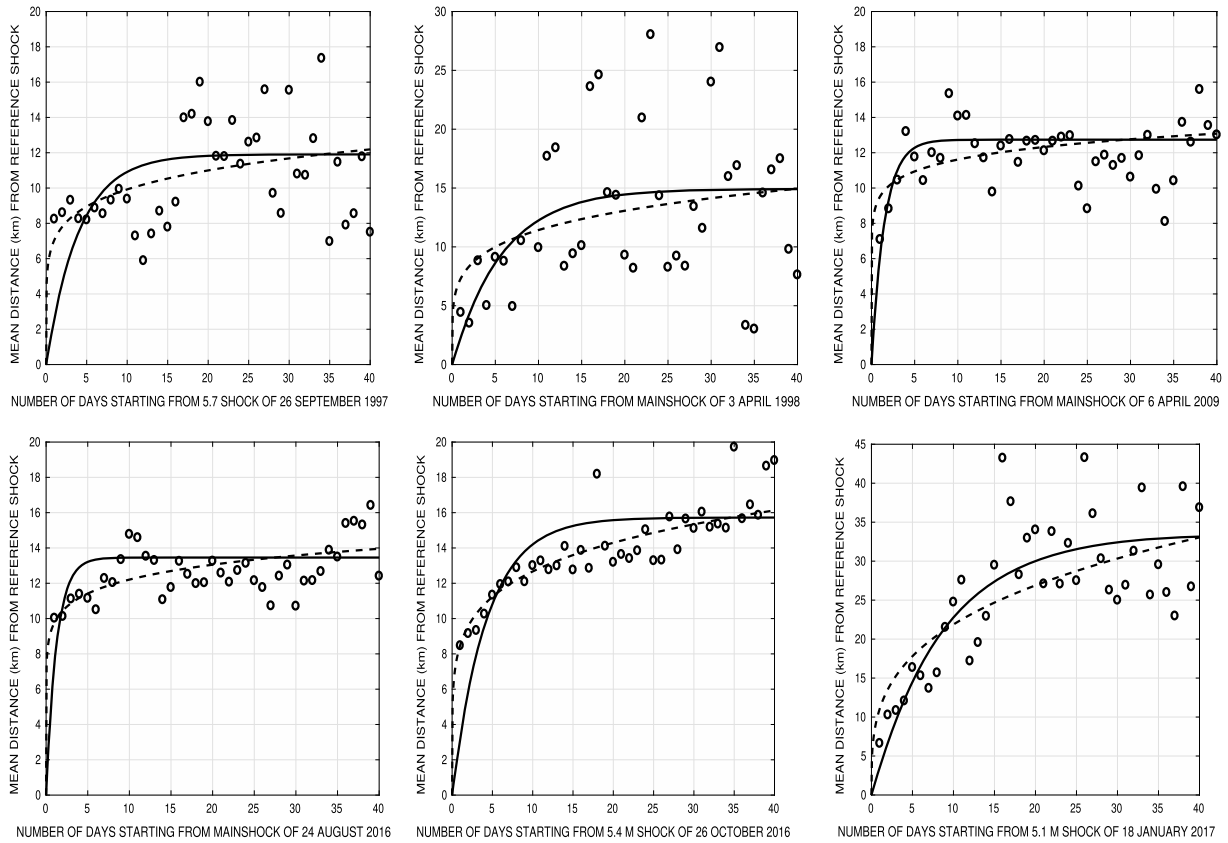

Figure 9. The results of the parametric analysis of aftershock migration for the first phase of the Colfiorito sequence (top left), the second phase of the Colfiorito sequence (top center), L'Aquila sequence (top right), the first phase of the Amatrice Visso-Norcia Campotosto sequence (bottom left), the second phase of the Amatrice Visso-Norcia Campotosto sequence (bottom center), and the third phase of the Amatrice Visso-Norcia Campotosto sequence (bottom right). The continuous (dashed) line corresponds to the exponential (power law) model fits.

to 3). As it clearly appears in the three curves, the values of the aftershock duration reported in Table 2 correspond to the first times after which the curves remain always below the threshold. In Table 2, we show the aftershock duration values for the three sequences, together with those from Valerio et al. (2017), obtained by the tangent method. As seen, the aftershock duration for the Colfiorito and Amatrice Visso-Norcia Campotosto sequences were very close to each other (difference less than 7%), while the L'Aquila aftershock sequence was more than 50% longer. We also notice that the values we estimated are close to those found

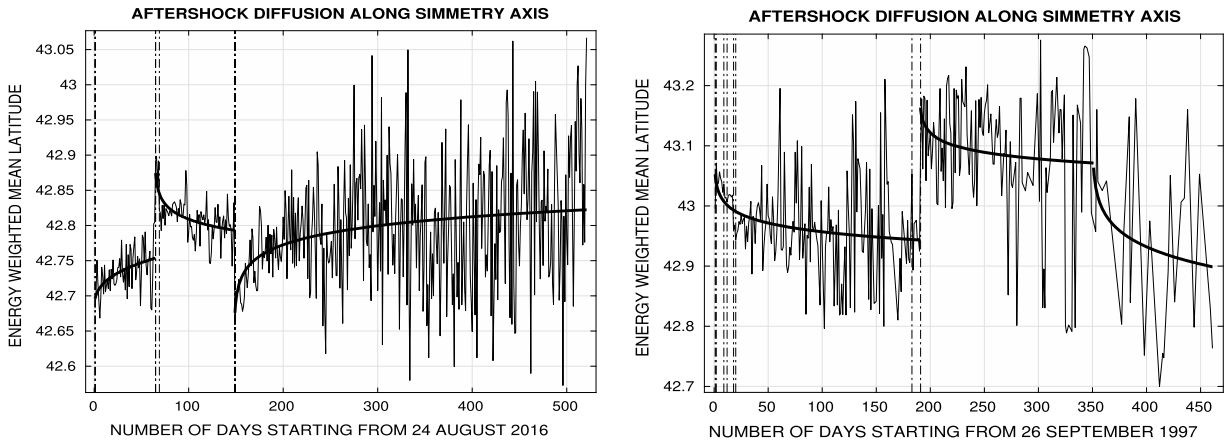

Figure 10. The results of the analysis of aftershock migration at sequence level. On the left (right), the Amatrice Visso-Norcia Campotosto (Colfiorito) sequence. The dashed vertical lines correspond to the occurrence of the events with $M \geq 5$.

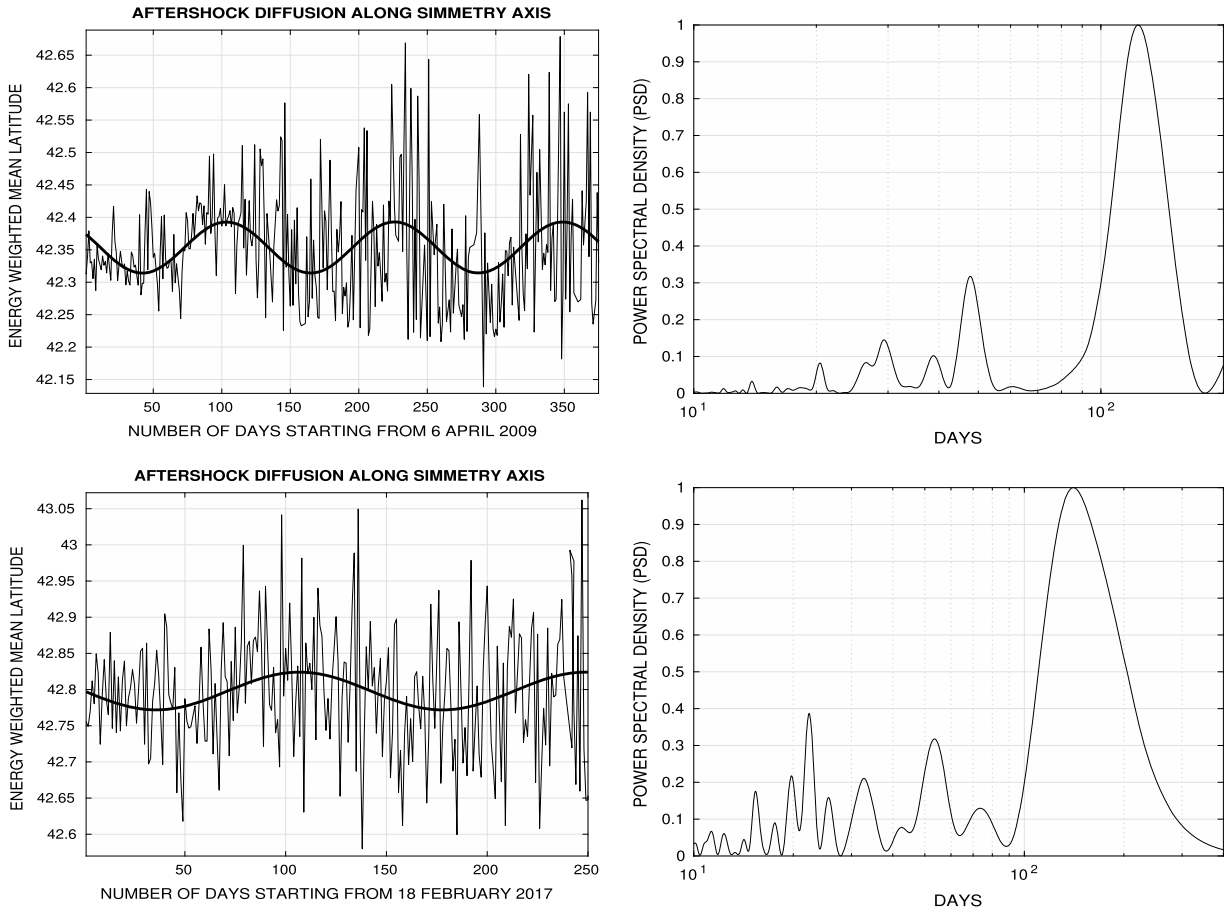

Figure 11. The results of the analysis of aftershock migration for the L'Aquila sequence (top) and the Campotosto sequence phase (bottom). (left) As in the previous figure but using a periodic model; the estimated period for the sinuosoidal model was 123 days approximately for the L'Aquila sequence and 141 days approximately for the Campotosto phase. (right) The periodogram computed from the data of the same sequences. The estimated period was 123 days ca for the L'Aquila sequence and 142 for the Campotosto phase.

by Valerio et al. (2017). However, the method used here has a strong statistical base. The values chosen for T were 250 days for the L'Aquila sequence and 60 days for the other two sequences.

4.2. Evolution of Aftershock Spatial Distribution

Two different types of parametric models, that is, exponential or power law, were applied to each of the six sequence phases. Fits are shown in Figure 9. We notice that for the L'Aquila sequence and the third phase of the Amatrice Visso-Norcia Campotosto one, the exponential model described better the initial evolution of aftershock migration. In fact, the ratio between the mean of the absolute value differences between the first 20 data points and the power law model to the same mean corresponding to the exponential model was 1.2 and 1.3, respectively. Instead, for the first and second phases of the Amatrice Visso-Norcia Campotosto sequence was the other way around since the values of this ratio were 0.7 and 0.4, respectively. The result for the first phase of the Colfiorito sequence was similar to these last two since the value of this ratio was 0.7. There were no differences between the two models in the case of the second phase of the Colfiorito sequence for which the value of this ratio was equal to 1.

The results for the analysis of aftershock migration at sequences level with parametric model are shown in Figure 10 for the Colfiorito and the Amatrice Visso-Norcia Campotosto sequence data sets, and in Figure 11 for the L'Aquila one, respectively (the dashed vertical lines correspond to the times of occurrence of events with $M \geq 5$). The L'Aquila sequence showed evidence of a simple periodic pattern. The period estimated for both the parametric model and the frequency domain approach was 123 days. Both the parametric model fit and the periodogram are shown in Figure 11.

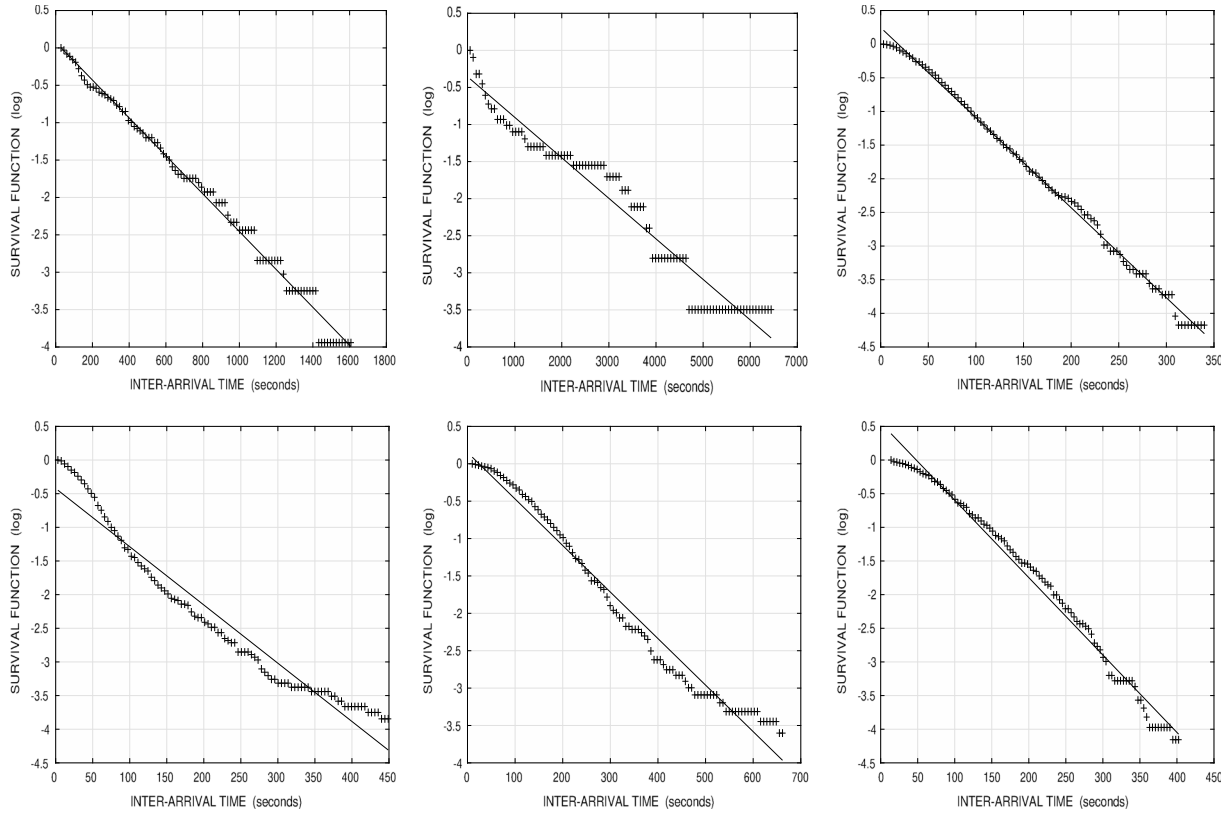

Figure 12. The estimated interarrival time survival function for the aftershocks occurred within the first 12 hr after: event 1 for the first phase of the Colfiorito sequence (top left), event 2 for the second phase of the Colfiorito sequence (top center), event 3 for the L'Aquila sequence (top right), event 4 for the first phase of the Amatrice Visso-Norcia Campotosto sequence (bottom left), event 5 for the second phase of the Amatrice Visso-Norcia Campotosto sequence (bottom center), and event 6 for the third phase of the Amatrice Visso-Norcia Campotosto sequence (bottom right).

Instead, the sequences of Amatrice Visso-Norcia Campotosto and Colfiorito displayed a piecewise continuous behavior.

In particular, the Amatrice Visso-Norcia Campotosto showed three phases:

(i) an initial northward aftershock migration until 26 October 2016 (Visso earthquake), when the activity jumped further north;
(ii) a following southward migration until 18 January 2017 (Campotosto earthquake), when the activity jumped further south; and
(iii) a northward aftershock migration similar to the first one, but showing larger random fluctuations.

Although this was a piecewise continuous time series, we performed frequency analysis obtaining a main peak in the periodogram at 137 days approximately. In addition, we performed both parametric periodic modeling and frequency analysis to the Campotosto sequence phase obtaining a period of 141 and 142 days approximately, respectively (see Figure 11). We point out that the seismic events of the Visso-Norcia phase remained in practice confined south of the Valnerina line. We finally notice that the spatial point of the first jump corresponds with good approximation to the intersection between the symmetry axis and the Ancona-Anzio line.

The Colfiorito sequence presented two phases:

(i) an initial southward aftershock migration lasting around 50 days followed by a almost flat trend with random fluctuation, until the 3 April 1998 shock when the activity jumped north and
(ii) a southward aftershock migration.

4.3. Distribution of Aftershock Interarrival Time

The estimates of the interarrival time survival function for the aftershocks of the six sequence phases are shown in Figure 12. From both visual inspection and the values of the normalized mean square error

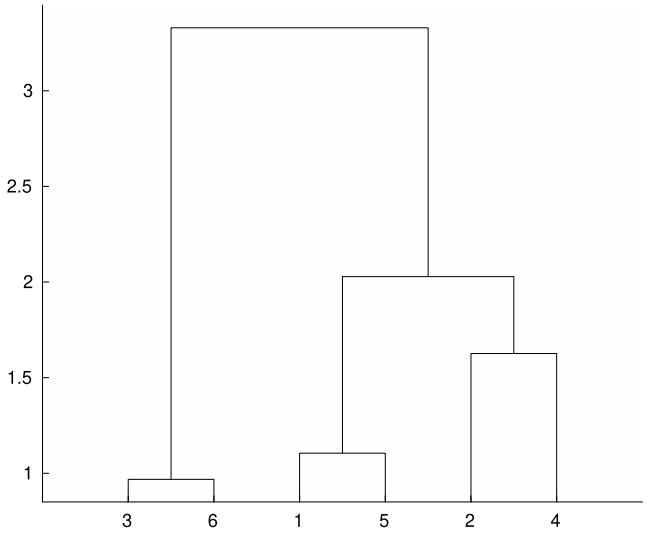

Figure 13. The dendrogram from the aftershock interarrival time results for each of the six sequence phases. The numbers corresponds to the phases: (1) Colfiorito first phase, (2) Colfiorito second phase, (3) L'Aquila, (4) Amatrice, (5) Visso-Norcia, and (6) Campotosto. Pairs of variables were used for clustering: normalized mean square error between data and estimated linear model; estimated value of the linear model proportionality constant. The clustering algorithm was driven by the Ward criterion, which minimizes the sum of intracluster variances, computed on the basis of the Euclidean distance.

between the data and the best linear fit of the six phases, we notice that for both the L'Aquila sequence and the third phase of the Amatrice Visso-Norcia Campotosto sequence there was a very good agreement between data and the exponential model, which can be derived theoretically for the event interarrival time of the standard Poisson process (Daley & Vere-Jones, 2003). We recall that Molchan (2005), under very general conditions, derived theoretically this model. For the remaining phases, the agreement was not so good; moreover, the estimated values of the proportionality constant of the linear model were noticeably smaller than those of the other two phases. By applying hierarchical clustering to the pairs of normalized mean square error and estimated linear model proportionality constant, as shown in Figure 13, we notice the appearance of the same two groups found by the first type of analysis of aftershock migration: the L'Aquila sequence and the last phase of the Amatrice Visso-Norcia Campotosto sequence in one and all the remaining four phases in the other one. The six sequence phases are indicated by the number of their reference event (see Table 1).

5. Concluding Remarks

The three sequences studied here occurred in a portion of central Italy characterized by the presence of crustal NE-SW striking cross structures, with regional extension. These lineaments, named Valnerina and Ancona-Anzio (e.g., Pizzi & Galadini, 2009, and references herein), are misoriented with respect to the present extensional stress (Carafa & Bird, 2016; see Figure 1). This is probably the reason why they have been showing low ability to produce strong magnitude events. In fact, no surface evidence for Quaternary faulting has been found so far and historical and instrumental seismicity has been showing only $M < 6$ events (Pizzi & Galadini, 2009). On the other hand, $M > 6.5$ events are more likely to occur along numerous NW-SE trending normal fault systems (Carafa et al., 2017). As claimed by Pizzi and Galadini (2009), the NE-SW trending lineaments could act as "persistent structure barriers," probably influencing the propagation and the segmentation of the active extensional faults along the axial zone of central Apennines. Moreover, the authors stated that these barriers would influence the length of the NW-SE active faults modulating their evolution through the crust.

In particular, Pizzi and Galadini (2009) noticed that the fault segments located less than 10 km from crustal tectonic lines are a few kilometers long and may display a dispersed and complex pattern, while fault segments located further from tectonic lines can grow radially and are longer (> 15 km).

The longest of these lineaments, that is, the "Ancona-Anzio," divides two completely different lithological and hydrogeological domains:

(i) On the southern side, a carbonate platform, mainly characterized by the outcropping of a thick permeable carbonatic (dolomitic in its lower part) sequence hosting a huge and regional groundwater circulation (karst environment, well represented by the Gran Sasso hydrostructure in the L'Aquila area with a total discharge of 23 m^3/s (Boni et al., 1986). Fissured carbonate rocks have a hydraulic conductivity in the range of 10^{-8}–10^{-7} m/s. Where the fracturing is more widespread owing to intense tectonic movements and/or where deep karstified areas and joints are present, hydraulic conductivity can also reach 10^{-6}–10^{-4} m/s (Monjoie, 1980).

(ii) On the northern side, a pelagic basin shows an alternation of permeable and impervious layers, each characterized by completely different values of hydraulic properties (i.e., conductivity). Accordingly, lithological and hydrogeological pattern is here more complex than the southern formation. The geological setting is composed by the sedimentary sequence termed Umbro-Marchigiana, characterized by thick (1.5–2 km) evaporitic layers (named Burano Formation) overlaid by a calcareous unit (limestones, marly limestones, and marls) and by a flysch unit, deposited during the uplift of the Apennine chain in that area. The evaporites, the terrigenous part of the carbonate sequence and the flysch, have hydraulic conductivity in the order of 10^{-10}–10^{-8} m/s, while much higher permeability 10^{-6}–10^{-4} m/s (Monjoie,

1980 for both ranges) characterizes the "pure" basal calcareous complex (as defined by Di Capua et al., 2016). Accordingly, hydrogeological setting in the upper deposits of that sequence is made up of multiple aquifers, that is, a series of aquifers separated from each other by confining layers acting as aquitards, while regional flow is only present where carbonates are present.

We recall that at "sequence" level, we observed a continuous and periodic aftershock migration pattern for the L'Aquila sequence. Conversely, the two sequences of Colfiorito and Amatrice Visso-Norcia Campotosto showed a piecewise continuous pattern. Furthermore, the aftershocks of the last two sequences lasted considerably less than in the L'Aquila sequence. A possible explanation of this different behavior is the following. We notice that the L'Aquila sequence took place well below the Ancona-Anzio line. Instead, the Colfiorito one was well above that line and the Amatrice Visso-Norcia Campotosto one was partially located both above and below the line. The different lithological and hydrogeological properties of the two regions below and above this line could influence the appearance of the two different patterns, as detailed in the interpretation of the sequence phase results. A further evidence to support this thesis is the periodic pattern observed in the Campotosto sequence phase, which took place on the same side of the L'Aquila sequence with respect to the "Ancona-Anzio" line. Furthermore, the presence of one of these lines in the area involved by seismic activity, as in the case of the Colfiorito and the Amatrice Visso-Norcia Campotosto sequences could also be relevant. In fact, they could not merely play a role as physical barriers, but they possibly have a strong influence on strain propagation. In particular, we suggest that these lines could perform a sort of energy rebound and increase instability along the fault itself, as well as on adjacent structures, where another mainshock can be so generated. In addition, we would like to notice the closeness between the period of the L'Aquila sequence (123 days), the one of the Campotosto sequence phase (141 days), and the location of the main peak in the periodogram of the discontinuous Amatrice Visso-Norcia Campotosto sequence (137 days). This could indicate the presence of a unique periodic factor influencing seismic activity.

Focusing on the "sequence phase" level, we notice that the group of sequence phases of L'Aquila and Campotosto exhibited an aftershock migration better described by an exponential model than by a power law one, while for the Amatrice, Visso-Norcia, and the 26 September 1997 Colfiorito sequence phases, a power law model was more suited than the exponential one. Moreover, for the first group, the aftershock interarrival time were very well fitted by an exponential model, whereas for the sequences of the other group, noticeable deviations from this model appeared. In order to formulate a possible explanation for the observed differences, we recall the interpretation given by Miller et al. (2004) for the aftershocks of the 26 September 1997 sequence. The Authors stated that this anomalous sequence, lasted more than 30 days, with thousands of aftershocks including four additional events with magnitudes between 5 and 6 was not well explained by elastic stress transfer only. Indeed, an additional "source" of pressure was necessary, which was identified by them in the CO_2 encountered beneath the Colfiorito region in deep drilling; the CO_2 was at near-lithostatic pressure. The same source was claimed to play a major role in the evolution of the aftershocks in the L'Aquila earthquake (Lucente et al., 2010; Terakawa et al., 2010). However, the effects of CO_2 gas trap at depth, are likely influenced by the local lithological settings, which is different between the regions above and below the Ancona-Anzio line, as described before in this section. Many researchers claim that evaporites act as a seal for rising deep-seated CO_2 (Chiodini et al., 2004) that can accumulate and, possibly, have an important role in triggering earthquakes. Therefore, the fact that the L'Aquila and Campotosto phases occurred well below the Ancona-Anzio line, while the remaining phases occurred well above or almost on it, could explain the different behavior observed between the two groups of sequence phases.

Acknowledgments
The catalog data used in this study are provided by the Istituto Nazionale di Geofisica e Vulcanologia (INGV) web services: ISIDe working group (2016) version 1.0, DOI: 10.13127/ISIDe, which is accessible at http://cnt.rm.ingv.it/en/iside website. The Colfiorito sequence data were extracted from the CSI 1.1 (1981–2002) catalog (Castello et al., 2006), available at http://csi.rm.ingv.it/ website. In Table 1, some basic information about the three data sets are shown. The authors are thankful to Michele Carafa and to the two reviewers for their very useful comments and suggestions. We wish to thank the INGV staff for their enormous effort in producing very high-quality seismic data of the huge Central Italy sequence; also, the INGV staff managing the web services is warmly acknowledged.

References

Amato, A., Azzara, R., Chiarabba, C., Cimini, G. B., Cocco, M., Di Bona, M., et al. (1998). The 1997 Umbria-Marche, Italy, earthquake sequence: A first look at the main shocks and aftershocks. *Geophysical Research Letters*, *25*(15), 2861–2864.

Barba, S., & Basili, R. (2000). Analysis of seismological and geological observations for moderate-size earthquakes: The Colfiorito Fault System (Central Apennines, Italy). *Geophysical Journal International*, *141*(1), 241–252.

Bath, M., & Duda, S. J. (1964). Earthquake volume, fault plane area, seismic energy, strain, deformation and related quantities. *Annals of Geophysics*, *17*(3), 353–368.

Boni, C., Bono, P., & Capelli, G. (1986). Schema idrogeologico dell'Italia Centrale. *Memorie della Società Geologica Italiana*, *35*(2), 991–1012. with hydrogeological map at 1:500,000 scale.

Caputo, M., & Sebastiani, G. (2011). Time and space analysis of two earthquakes in the Appennines (Italy). *Natural Sciences*, *3*(9), 768–774. https://doi.org/10.4236/ns.2011.39101

Carafa, M. M. C., & Bird, P. (2016). Improving deformation models by discounting transient signals in geodetic data: 2. Geodetic data, stress directions, and long-term strain rates in Italy. *Journal of Geophysical Research: Solid Earth*, *121*, 5557–5575. https://doi.org/10.1002/2016JB013056

Carafa, M. M. C., Valensise, G., & Bird, P. (2017). Assessing the seismic coupling of shallow continental faults and its impact on seismic hazard estimates: A case-study from Italy. *Geophysical Journal International*, *209*(1), 32–47. https://doi.org/10.1093/gji/ggx002

Castello, B., Selvaggi, G., Chiarabba, C., & Amato, A. (2006). CSI Catalogo della sismicità Italiana 1981–2002. versione 1.1, INGV-CNT, Roma.

Chiaraluce, L., Amato, A., Cocco, M., Chiarabba, C., Selvaggi, G., Di Bona, M., et al. (2004). Complex normal faulting in the Apennines thrust-and-fold belt: The 1997 seismic sequence in central Italy. *Bulletin of the Seismological Society of America*, *94*(1), 99–116. https://doi.org/10.1785/0120020052

Chiaraluce, L., Di Stefano, R., Tinti, E., Scognamiglio, L., Michele, M., Casarotti, E., et al. (2017). The 2016 central Italy seismic sequence: A first look at the mainshocks, aftershocks, and source models. *Seismological Research Letters*, *88*(3), 757–771. https://doi.org/10.1785/0220160221

Chiaraluce, L., Valoroso, L., Piccinini, D., Di Stefano, R., & De Gori, P. (2011). The anatomy of the 2009 L'Aquila normal fault system (central Italy) imaged by high resolution foreshock and aftershock locations. *Journal of Geophysical Research*, *116*, B12311. https://doi.org/10.1029/2011JB008352

Chiodini, G., Cardellini, C., Amato, A., Boschi, E., Caliro, S., Frondini, F., & Ventura, G. (2004). Carbon dioxide Earth degassing and seismogenesis in central and southern Italy. *Geophysical Research Letters*, *31*, L07615. https://doi.org/10.1029/2004GL019480

Ciaccio, M. G., Barchi, M. R., Chiarabba, C., Mirabella, F., & Stucchi, E. (2005). Seismological, geological and geophysical constraints for the Gualdo Tadino fault, Umbria-Marche Apennines (Central Italy). *Tectonophysics*, *406*(3-4), 233–247.

Daley, D. J., & Vere-Jones, D. (2003). An introduction to the theory of point processes (2nd ed.)., (Vol. I, pp. xxii+469). New York: Springer-Verlag.

Deschamps, A., Courboulex, F., Gaffet, S., Lomax, A., Virieux, J., Amato, A., et al. (2000). Spatio-temporal distribution of seismic activity during the Umbria-Marche crisis, 1997. *Journal of Seismology*, *4*(4), 377–386. https://doi.org/10.1023/A:1026568419411

Di Capua, G., Peppoloni, S., Amanti, M., Cipolloni, C., & Conte, G. (2016). Site classification map of Italy based on surface geology, *Engineering geology special publications* (Vol. 27, pp. 147–158). London: Geological Society. https://doi.org/10.1144/EGSP27.13

Di Giovambattista, R., & Tyupkin, Y. S. (2000). Spatial and temporal distribution of seismicity before the Umbria-Marche September 26, 1997 earthquakes. *Journal of Seismology*, *4*, 589–598.

Di Luccio, F., Ventura, G., Di Giovambattista, R., Piscini, A., & Cinti, F. R. (2010). Normal faults and thrusts reactivated by deep fluids: The 6 April 2009 M_W 6.3 l'Aquila earthquake, central Italy. *Journal of Geophysical Research*, *115*, B06315. https://doi.org/10.1029/2009JB007190

Galli, P., & Galadini, F. (1999). Seismotectonic Framework of the 1997-1998 Umbria-Marche (Central Italy) earthquakes. *Seismological Research Letters*, *70*(4), 417–461.

Galli, P., Peronace, E., Bramerini, F., Castenetto, S., Naso, G., Cassone, F., & Pallone, F. (2016). The MCS intensity distribution of the devastating 24 August 2016 earthquake in central Italy (M_W 6.2). *Annals of Geophysics*, *59*. Fast Track 5, 1–13, https://doi.org/10.4401/ag-7287

Gasparini, C., De Rubeis, V., Maramai, A., & Murru, M. (1993). The November 23, 1980 Irpinia earthquake: An analysis with the new procedure of intensity evaluation. *Annals of Geophysics*, *36*(5-6), 35–46.

Gentili, S., Di Giovambattista, R., & Peresan, A. (2017). Seismic quiescence preceding the 2016 central Italy earthquakes. *Physics of The Earth and Planetary Interiors*, *272*, 27–33. https://doi.org/10.1016/j.pepi.2017.09.004

Hastie, T. J., & Tibshirani, R. J. (1990). *Generalized additive models*. New York-Washington, DC: Chapman & Hall.

Lehmann, E. L. (1998). *Elements of large-sample theory*. New York: Springer texts in statistics, Springer Verlag.

Lucente, F. P., De Gori, P., Margheriti, L., Piccinini, D., Di Bona, M., Chiarabba, C., & Piana Agostinetti, N. (2010). Temporal variation of seismic velocity and anisotropy before the 2009 M_W 6.3 L'Aquila earthquake, Italy. *Geology*, *38*(11), 1015. https://doi.org/10.1130/G31463.1

Malagnini, L., Lucente, F. P., De Gori, P., Akinci, A., & Munafò, I. (2012). Control of pore fluid pressure diffusion on fault failure mode: Insights from the 2009 l'aquila seismic sequence. *Journal of Geophysical Research*, *117*, B05302. https://doi.org/10.1029/2011JB008911

Marzorati, S., Cattaneo, M., Frapiccini, M., Monachesi, G., & Ladina, C. (2016). Recent seismicity before the 24 August 2016 MW 6.0 central Italy Earthquake as recorded by the ReSIICO seismic network. *Annals of Geophysics*, *59*. Fast Track 5, 1–12, https://doi.org/10.4401/ag-7191

Miller, S. A., Collettini, C., Chiaraluce, L., Cocco, M., Barchi, M., & Kaus, B. J. P. (2004). Aftershocks driven by a high-pressure CO_2 source at depth. *Nature*, *427*, 724–727. https://doi.org/10.1038/nature02251

Molchan, G. (2005). Interevent time distribution in seismicity: A theoretical approach. *Pure and Applied Geophysics*, *162*(6-7), 1135–1150.

Monjoie, A. (1980). Prevision et controle des caractristiques hydrogeologiques dans les tunnels du Gran Sasso (Appenin, Italie) [Prediction and control of the hydrogeological characteristics of the Gran Sasso tunnel (Apennines, Italy)]. In L. Calembert (Ed.), *LIvre Jubilaire* (pp. 209–229). Liége: Thone.

Nur, A., & Booker, J. R. (1972). Aftershocks caused by pore fluid flow? *Science*, *175*(4024), 885–887.

Pizzi, A., & Galadini, F. (2009). Pre-existing cross-structures and active fault segmentation in the northern-central Apennines (Italy). *Tectonophysics*, *476*(1), 304–319. https://doi.org/10.1016/j.tecto.2009.03.018

Ripepe, M., Piccinini, D., & Chiaraluce, L. (2000). Foreshock sequence of september 26th, 1997 Umbria-Marche earthquakes. *Journal of Seismology*, *4*(4), 387–399.

Rovida, A., Locati, M., Camassi, R., Lolli, B., & Gasperini, P. (Eds.) (2016). *Italian parametric earthquake catalogue (Catalogo Parametrico dei Terremoti Italiani) Edited by* Rovida, A., Locati, M., Camassi, R., Lolli, B., & Gasperini, P. Rome, Italy: Istituto Nazionale di Geofisica e Vulcanologia. version CPTI15 release 1.5.

Saichev, A., & Sornette, D. (2007). Theory of earthquake recurrence times. *Journal of Geophysical Research*, *112*, B04313. https://doi.org/10.1029/2006JB004536

Schuster, A. (1906). The periodogram and its optical analogy. *Proceedings of the Royal Society A: Mathematical, Physical and Engineering Sciences*, *77*, 136–140. https://doi.org/10.1098/rspa.1906.0011

Scognamiglio, L., Tinti, E., Casarotti, E., Pucci, S., Villani, F., Cocco, M., et al. (2018). Complex fault geometry and rupture dynamics of the MW 6.5, 30 October 2016, Central Italy earthquake. *Journal of Geophysical Research: Solid Earth*, *123*, 2943–2964. https://doi.org/10.1002/2018JB015603

Selvaggi, G., & Amato, A. (1992). Subcrustal earthquake in northern Appennines (Italy): Evidence for a still active subduction? *Geophysical Research Letters*, *19*(21), 2127–2130.

Serra, J. (1982). *Image analysis and mathematical morphology*. London: Academic Press Inc.

Spassiani, I., & Sebastiani, G. (2016). Magnitude-dependent epidemic-type aftershock sequences model for earthquakes. *Physical Review E*, *93*, 042134. https://doi.org/10.1103/PhysRevE.93.042134

Terakawa, T., Zoporowski, A., Galvan, B., & Miller, S. A. (2010). High-pressure fluid at hypocentral depths in the L'Aquila region inferred from earthquake focal mechanisms. *Geology*, *38*(11), 995–998. https://doi.org/10.1130/G31457.1

Toda, S., & Stein, R. S. (2018). Why aftershock duration matters for probabilistic seismic hazard assessment. *Bulletin of the Seismological Society of America*, *108*(3A), 1414–1426.

Valerio, E., Tizzani, P., Carminati, E., & Doglioni, C. (2017). Longer aftershocks duration in extensional tectonic settings. *Scientific Reports*, *7*(1), 16403. https://doi.org/10.1038/s41598-017-14550-2

Valoroso, L., Chiaraluce, L., Piccinini, D., Di Stefano, R., Schaff, D., & Waldhauser, F. (2013). Radiography of a normal fault system by 64,000 high-precision earthquake locations: The 2009 L'Aquila (central Italy) case study. *Journal of Geophysical Research: Solid Earth*, *118*, 1156–1176. https://doi.org/10.1002/jgrb.50130

Vuan, A., Sugan, M., Chiaraluce, L., & Di Stefano, R. (2017). Loading rate variations along a midcrustal shear zone preceding the Mw6.0 earthquake of 24 August 2016 in Central Italy. *Geophysical Research Letters*, *44*, 12,170–12,180. https://doi.org/10.1002/2017GL076223

Ward, J. H. (1963). Hierarchical grouping to optimize an objective function. *Journal of the American Statistical Association*, *58*(301), 236–244.

Ziv, A. (2006). Does aftershock duration scale with mainshock size? *Geophysical Research Letters*, *33*, L17317. https://doi.org/10.1029/2006GL027141